OPEN

The ISME Journal (2017), 1–14
© 2017 International Society for Microbial Ecology All rights reserved 1751-7362/17
www.nature.com/ismej

ORIGINAL ARTICLE

Bacteria isolated from lung modulate asthma susceptibility in mice

Aude Remot[1], Delphyne Descamps[2], Marie-Louise Noordine[1], Abdelhak Boukadiri[3], Elliot Mathieu[1], Véronique Robert[1], Sabine Riffault[2], Bart Lambrecht[4,5], Philippe Langella[1], Hamida Hammad[4,5] and Muriel Thomas[1]

[1]*Micalis Institute, INRA, AgroParisTech, Université Paris-Saclay, Jouy-en-Josas, France;* [2]*VIM, INRA, Université Paris-Saclay, Jouy-en-Josas, France;* [3]*Animal Genetics and Integrative Biology (UMR1313, GABI), INRA-AgroParisTech, Jouy-en-Josas, France;* [4]*Inflammation Research Center, VIB, Ghent, Belgium and* [5]*Department of Respiratory Medicine, Ghent University, Ghent, Belgium*

Asthma is a chronic, non-curable, multifactorial disease with increasing incidence in industrial countries. This study evaluates the direct contribution of lung microbial components in allergic asthma in mice. Germ-Free and Specific-Pathogen-Free mice display similar susceptibilities to House Dust Mice-induced allergic asthma, indicating that the absence of bacteria confers no protection or increased risk to aeroallergens. In early life, allergic asthma changes the pattern of lung microbiota, and lung bacteria reciprocally modulate aeroallergen responsiveness. Primo-colonizing cultivable strains were screened for their immunoregulatory properties following their isolation from neonatal lungs. Intranasal inoculation of lung bacteria influenced the outcome of allergic asthma development: the strain CNCM I 4970 exacerbated some asthma features whereas the pro-Th1 strain CNCM I 4969 had protective effects. Thus, we confirm that appropriate bacterial lung stimuli during early life are critical for susceptibility to allergic asthma in young adults.
The ISME Journal advance online publication, 3 January 2017; doi:10.1038/ismej.2016.181

Introduction

Allergic asthma is a worldwide problem with rising prevalence and morbidity in industrialized countries. Variable airway obstruction is a typical feature of this disease, caused by chronic eosinophilic airway inflammation, mucus overproduction, airway wall remodeling and bronchial hyperactivity. In allergic asthma, allergen-specific Th2 lymphocytes cause inflammation and control the synthesis of allergen-specific IgE, a hallmark of allergic sensitization (Kool *et al.*, 2012; Plantinga *et al.*, 2013; Just *et al.*, 2014). The cause of the asthma epidemic in the Western world is unclear, but its increased incidence has been correlated to changes in environment and gut microbiota (Fujimura and Lynch, 2015).

It has been proposed that the perturbation of early microbial stimulation in industrialized countries, due to improved hygiene, excessive antibiotherapy and dietary changes, results in an aberrant immune response to innocuous antigens later in life (Wills-Karp *et al.*, 2001; Noverr and Huffnagle, 2005; Schuijs *et al.*, 2015). However, the gut dysbiosis observed in asthma did not obligatory mean a causal role of gut microbiota in the pathology. Recent epidemiological and clinical data (Hoskin-Parr *et al.*, 2013), as well as experimental data obtained in mouse models (Noverr *et al.*, 2004; Olszak *et al.*, 2012), support the key role of the microbial environment. Bacterial colonization of the gut during the first months of life is critical for the development and the balance of the immune system: it promotes the maturation of the epithelial mucosa (Cherbuy *et al.*, 2010; Tomas *et al.*, 2013, 2015), the establishment of immune tolerance (Gaboriau-Routhiau *et al.*, 2009; Cahenzli *et al.*, 2013) and improves stimulation of the immune system that helps to prevent and/or resolve infectious diseases (Cerf-Bensussan and Gaboriau-Routhiau, 2010; De Filippo *et al.*, 2010; Buffie and Pamer, 2013).

Healthy lungs have historically been considered to be sterile, but the description of a resident lung microbiota emerged a few years ago and broke this dogma. A bacterial community has been described in healthy human lungs (Charlson *et al.*, 2011; Erb-Downward *et al.*, 2011). Lung bacteria originate from the upper respiratory tract and the mouth (Bassis *et al.*, 2015; Venkataraman *et al.*, 2015). The question of a stable versus transient colonization of lung by bacteria remains open (Segal *et al.*, 2013), but even if the lung microbes are only transited they

Correspondence: A Remot or M Thomas, Laboratoire Interactions hôtes-commensaux et probiotiques, UMR 1319 Micalis, INRA, Domaine de Vilvert, 78350 Jouy-en-Josas, France–AgroParisTech, UMR 1319 Micalis, 78350 Jouy-en-Josas, France.
E-mail: aude.remot@inra.fr or muriel.thomas@inra.fr
Received 11 May 2016; revised 3 November 2016; accepted 11 November 2016

can have major health impact. The composition and role of the lung microbiota remain largely unknown, and has mainly been explored using genomic approaches (Beck *et al.*, 2012; Charlson *et al.*, 2012). In 2011, Sibley *et al.* evaluated the cultivability of the airway microbiome using culture-enriched molecular profiling and were able to cultivate 43 of the 48 families detected by deep sequencing. Using both culture and genomic approaches, Yun *et al.* (2014) have shown that the lung microbiota is diversified through different environmental conditions and affects lung architecture. The direct contribution of the lung microbiota, and potential associated dysbiosis, in both the physiology and pathology of the respiratory tract remains unclear.

Recent publications suggest that the lung microbiota is altered in asthmatic patients. Analysis of 16s RNA sequences in bronchial lavage from asthmatic children revealed a highly significant increase of *Proteobacteria* (Hilty *et al.*, 2010). Moreover, airway dysbiosis appears to vary depending on the severity of the disease (Huang *et al.*, 2015) or corticosteroid responsiveness (Goleva *et al.*, 2013). The correlation between asthma and modification of the airway microbiota composition is now clearly established (Teo *et al.*, 2015; Smits *et al.*, 2016). Gollwitzer *et al.* (2014) demonstrated that microbial signals in the lung of neonatal mice clearly improve immune tolerance to House Dust Mite (HDM) allergens via PD-1/PD-L1 signaling in regulatory T cells and dendritic cells (DC). Their study established a direct contribution of microbial components to HDM induced asthma.

Previous studies proposed that asthma features are influencing by microbiota based on ovalbumin challenge model (Herbst *et al.*, 2011; Olszak *et al.*, 2012) or oral antibiotic treatment (Hill *et al.*, 2012). The contribution of lung bacterial strains to the establishment of asthma or their participation in chronic inflammation has never been addressed by using HDM challenge. In this study, we demonstrate that lung bacteria participate in determining the immune and inflammatory responses to HDM in neonatal C57BL/6 mice.

Materials and methods

Bacterial strains, media, growth conditions

Lung bacterial strains were isolated from mouse lung homogenates prepared using an Ultraturax or Tissue Lyser (Qiagen, Courtaboeuf, France), diluted in Brain Heart Infusion liquid medium supplemented with 5 g l^{-1} of yeast extract, 5 mg l^{-1} of hemin, 2 mg l^{-1} of vitamin K1 and 0.5 g l^{-1} of cysteine (yhBHI, all products are from Sigma-Aldrich, Eurogenetec, Angers, France) and cultivated on agar yhBHI medium (GyhBHI), M17, MRS or Mannitol Sel Agar medium for 24–48 h at 37 °C under aerobic conditions or 5 days at 37 °C in a Freter chamber under anaerobic conditions. Isolated strains were frozen at −80 °C in 16% glycerol. Strain identities were confirmed by mass spectrometry, API gallery (Biomérieux, Craponne, France) and 16S PCR sequencing. Selected strains were deposited at the French National Collection of Microorganism Cultures (CNCM) under the name CNCM I 4969 and CNCM I 4970 (patented strains).

Animals and procedures

Animal experiments were approved by the local ethics committee under the registration number 01553.01. SPF C57BL/6 mice purchased from Janvier (Le Genest, St Isle, France) were bred and housed under FELASA SPF conditions in our animal facilities (IERP, INRA, Jouy-en-Josas, France, or VIB, Ghent, Belgium). GF C57BL/6 mice were purchased from CDTA (CNRS, Orleans, France) or local breeders (INRA) and were bred and housed under germ-free conditions in Trexler-type isolators (La Calhène, Vélizy, France) in the Anaxem animal facilities (INRA). For HDM allergic asthma induction, 7-day-old pups received 1 μg of HDM (Greer, Lenoir, NC, USA) or diluent lipopolysaccharide-free phosphate-buffered saline (PBS) (Lonza, Levallois-Perret, France) in a volume of 10 μl. They were challenged 1 week later with 10 μg of HDM (or PBS) for five consecutive days. In some experiments, 5-day-old pups received 1×10^6 bacteria in 10 μl PBS every 2 days.

Sample collection

Mice were killed by intraperitoneal injection of a lethal dose of ketamine and xylazine. The left bronchus was clamped and bronchoalveolar lavage (BAL) was performed on the right lobes with PBS 1 mM EDTA as described (Roux *et al.*, 2011). BAL supernatants were stored frozen at −20 °C and BAL cells were cytocentrifuged (Cytospin 5) on microscope slides (Superfrost, Thermo Scientific, Braunschweig, Germany), and then stained with May-Grünwald and Giemsa. The right lobe was used for flow cytometry or bacterial enumeration on agar plates after homogenization with a Tissue Lyser. For flow cytometry, the right lobe and the respiratory lymph nodes (RLN) (cervical, maxillary and mediastinal LN) were treated with 1 mg ml^{-1} collagenase D and 0.5 mg ml^{-1} DNAse I for cell isolation. The left lobe of the lung was kept frozen at −80 °C until processing for RNA extraction. For histological examination, the lungs were fixed with 4% paraformaldehyde and embedded in paraffin.

Precision-cut lung slides

Precision-cut lung slides (PCLS) were obtained from fresh lungs using a Krumdieck tissue slicer MD 6000 (Alabama Research and Development, Munford, AL, USA). The lungs were filled via the trachea with

RPMI 1.5% low melting point agarose (Invitrogen, Villebon sur Yvette, France) warmed to 37 °C. After 1 min for solidification, the lungs were placed in the microtome chamber of the Krumdieck, filled with cold PBS and cut at a thickness of 200 μm. Two PCLS per well were then placed at 37 °C, 5% CO_2, in P24 well plates (Nunc, Sigma-Aldrich, Lyon, France) with 1 ml RPMI 1640 (Gibco, Sigma-Aldrich, Lyon, France) supplemented with 10% heat inactivated fetal calf serum (Gibco) and 2 mM L-glutamine (Gibco). The medium was changed every 30 min during 2 h to remove the low melting point agarose and one last time after overnight incubation. PCLS were then co-incubated for 24 h with lung bacteria. Viability was assessed by measuring lactate dehydrogenase release (Sigma) or by MitoTracker Deep Red (ThermoFisher, Illkirch, France) labeling.

Histology
Five-micrometer lung sections were stained with hematoxylin/eosin/saffron or periodic acid schiff/alcian blue and photographed using CaseViewer software (3DHISTECH, Budapest, Hungary).

Gene expression by quantitative reverse transcriptase PCR
Total RNA was extracted from mouse lung homogenates using the NucleoSpin RNA kit (Macherey Nagel, Düren, Germany) and reverse transcribed using random primers and 50 U of Reverse Transcriptase (High-Capacity cDNA Archive Kit; Applied Biosystems by Life Technologies SAS, Villebon Sur Yvette, France) according to the manufacturer's instructions. The primers (Sigma-Aldrich) are listed in Supplementary Table S1. Quantitative reverse transcriptase PCR was performed in triplicate for each gene using an AbiPrism 7000 (Applied Biosystem) and Takyon ROx SYBR MasterMix (Eurogenetec) and the data were analyzed using 700 System SDS software (Applied Biosystem) to determine the cycle threshold (Ct) values. Messenger RNA (mRNA) expression was calculated using the ΔCt method and normalized to the expression of mHPRT.

Flow cytometry
After saturation with anti-CD32/CD16, cells were incubated with mAbs reactive to mPDCA1 (JF05-1C2.4.1, conjugated to FITC), MHCII (IA/IE, 2G9 or M5/114.15.2, FITC or PE), CD103 (M290 or 145-2D11, PE), CD86 (GL1, FITC), CD11b (M1/70, PerCP Cy5.5) or CD11c (HL3, Biotin or BV786). For T-cell staining, cells were incubated with mAbs reactive to CD4 (L3T4 or RM4-5, FITC or PECy7), CD45.2 (104, A780), CD3 (145-2C11, PerCP Cy5.5) or CD8 (Ly2, 53-6.8, Biotin or APC). For B-cell staining, cells were incubated with mAbs reactive to CD19 (1D3, APC), B220 (RA36B2, APC), CD45.2 (104, A780), CD5 (53-7.3, BV421) or CD23 (B3B4, FITC). All mAbs were purchased from BD Biosciences (San Jose, CA, USA) except for mPDCA1 (Miltenyi Biotec, Paris, France). APC-conjugated streptavidin (BD Biosciences) was used to label biotin Abs. At least 2×10^6 events were acquired using an Accuri or Fortessa FACS (BD Biosciences) and analyzed using FlowJo Sofware v7.5 (Tree Star Inc., Ashland, OR, USA).

Cytokine and Ig enzyme-linked immunosorbent assay
The cytokines IL-5, IL-10, IL-12p70, IL-17a or IFNγ (Mabtech, Nacka Strand, Sweden) and TSLP (eBiosciences, Paris, France) were quantified by enzyme-linked immunosorbent assay according to the manufacturer's instructions. Individual mouse sera were assayed for IgE and IgG1 (eBiosciences) according to the manufacturer's instructions.

Statistical analysis
Non-parametric Mann–Whitney (comparison of two groups, $n \geqslant 4$) or ANOVA Tukeys multiple comparison test (>2 groups) was used to compare unpaired values (GraphPadPrism software, GraphPad Software, Inc., San Diego, CA, USA). Significance is represented: $^{*}P<0.05$; $^{**}P<0.01$; $^{***}P<0.001$; and $^{****}P<0.0001$.

Results

Allergic asthma is not modified in germ-free mice
Asthma sensitivity was evaluated both in Germ-Free (GF) and Specific-Pathogen-Free (SPF) neonatal mice (Figure 1a). On day 0, 7-day-old neonates were intranasally sensitized with 1 μg of HDM or PBS diluent (PBS). They were challenged 1 week later with 10 μg of HDM or PBS intranasally on five consecutive days. All mice were killed, when they were 23 days old (5 days after the last challenge dose) to assess the inflammatory and immune responses in young adults (Figures 1b–d). *In vivo* lung function measurements were not feasible at that age. Both GF and SPF HDM challenged mice showed similar levels of inflammatory cell recruitment near the airway, bronchus epithelium thickening and myofibroblasts by hematoxilin eosin safran coloration of lung sections (Figure 1b). We did not observe any striking differences in lung structure, airway epithelium thickness or bronchus number between GF PBS- and SPF PBS-treated mice (Figure 1b), although the lungs of GF mice seemed to have fewer, larger alveoli, as previously published (Yun *et al.*, 2014). The total number of cells recovered from BAL was greater after HDM treatment (Figure 1c, PBS vs HDM: $P<0.05$ for GF; $P<0.01$ for SPF). We observed a type 2 immune (T2) signature after HDM treatment, as shown by the presence of eosinophils and IL-5 in BAL (Figure 1c, PBS vs HDM: $P<0.01$ for both GF and SPF), IgE in sera (Figure 1c, PBS vs HDM: $P<0.05$ for GF, $P<0.01$ for SPF), and IL-5 and IL-10

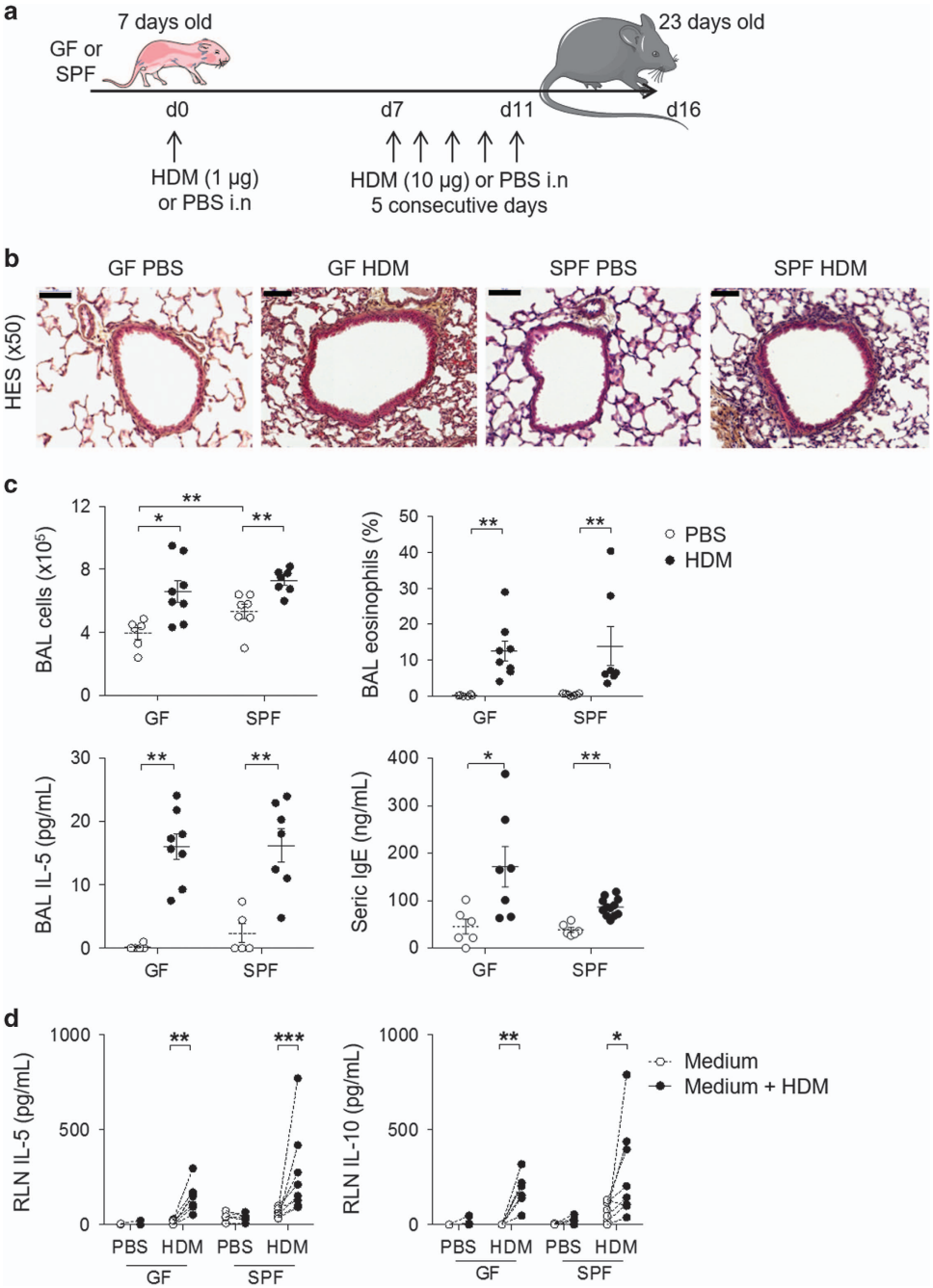

Figure 1 HDM-induced asthma is not exacerbated in GF mice. (**a**) Schematic outline of the experimental approach. Animals were killed on d16. (**b**) Lungs were fixed, embedded in paraffin and sectioned at a thickness of 5 µm. Lung sections were stained with hematoxylin–eosin–saffron (HES) and photographed using Case Viewer software. One representative section per group is shown ($n=6$ GF mice, $n=11$ SPF mice). The scale bar represents 50 µm. (**c**) BAL cells were enumerated, cytocentrifuged and stained with May–Gründwald–Giemsa. Eosinophils were enumerated and expressed as the percentage of total BAL cells. BAL IL-5 and serum IgE levels were measured by enzyme-linked immunosorbent assay (ELISA). Data are shown individually and as the mean ± s.e.m. (**d**) Individual respiratory lymph node (RLN) cells were isolated and cultivated 72 h in RPMI with or without HDM. IL-5 and IL-10 levels in the supernatants were measured by ELISA. The RPMI ± HDM values for the same mice are connected with a dotted line. Data are shown individually and as the mean ± s.e.m. (**a–d**) All data represent one of two independent experiments ($n=4$–8 mice per group).

secretion by RLN cells re-stimulated *in vitro* with RPMI medium supplemented with HDM (Figure 1d, $P<0.01$ (both) for GF; $P<0.001$ (IL-5) and $P<0.05$ (IL-10) for SPF). HDM efficiently induced allergic asthma, with an equivalent magnitude of T2 immunity and inflammatory response in GF and SPF mice, despite higher variability of IgE levels in GF sera.

We observed that some innate genes showed different patterns of expression at steady state

between GF and SPF mice: the level of *TSLP* mRNA was higher in GF mice, whereas *IL-10*, *IFNγ*, *CCL11* and *Muc5AC* mRNA levels were higher in SPF mice (Supplementary Figure S1, $P<0.05$ for IL-10, $P<0.01$ for all other genes). We next evaluated the number of lung immune cells, such as DC, T and B cells, by flow cytometry (Supplementary Figures S2A–D). All subpopulations of DCs, including plasmacytoid DCs (pDC) and the two subsets of conventional DCs (cDC) $CD11b^+$ $CD103^-$ ($CD11b^+$) and $CD11b^-$ $CD103^+$ ($CD103^+$), were present at the same levels in both GF and SPF lungs. The levels were also similar for CD4 and CD8 T cells, and B cells.

Altogether, our results show differences in mRNA levels for some innate genes between GF and SPF mice, but no marked differences of lung physiology or immune cell numbers (except for higher BAL cellularity for SPF mice, Figure 1c, $P<0.01$). HDM-induced allergic asthma was neither reduced nor exacerbated in GF mice. The absence of bacteria had no obvious influence on HDM pathology.

Asthma influences lung microbiota during the neonatal period

We tested whether HDM-induced asthma influences the viable bacteria amount in the lung. We used samples from embryonic day 19.5 and GF mice as sterile controls for our culture protocol. After birth, bacteria gradually arrived to the lung (Figure 2a). The bacteria can be cultivated both in aerobic and anaerobic conditions (data not shown). We never obtained cultivable bacteria from individual BAL of SPF neonatal mice (Figure 2a) nor purified enough bacterial DNA for 16S sequencing (data not shown). We succeeded in recovering viable bacteria from the lungs of SPF mice starting from 3 days after birth, and the number of lung bacteria increased significantly each week until weaning after 21 days (Figure 2a; $P<0.01$ and $P<0.001$). We isolated more than 20 bacterial strains from neonatal lungs: a majority of members within the Firmicutes phylum (*Staphylococcus*, *Streptococcus*, *Enterococcus*, *Listeria, Lactobacillus*) and some from the Proteobacteria phylum (*Escherichia coli*, *Proteus mirabilis*) (Supplementary Table S2).

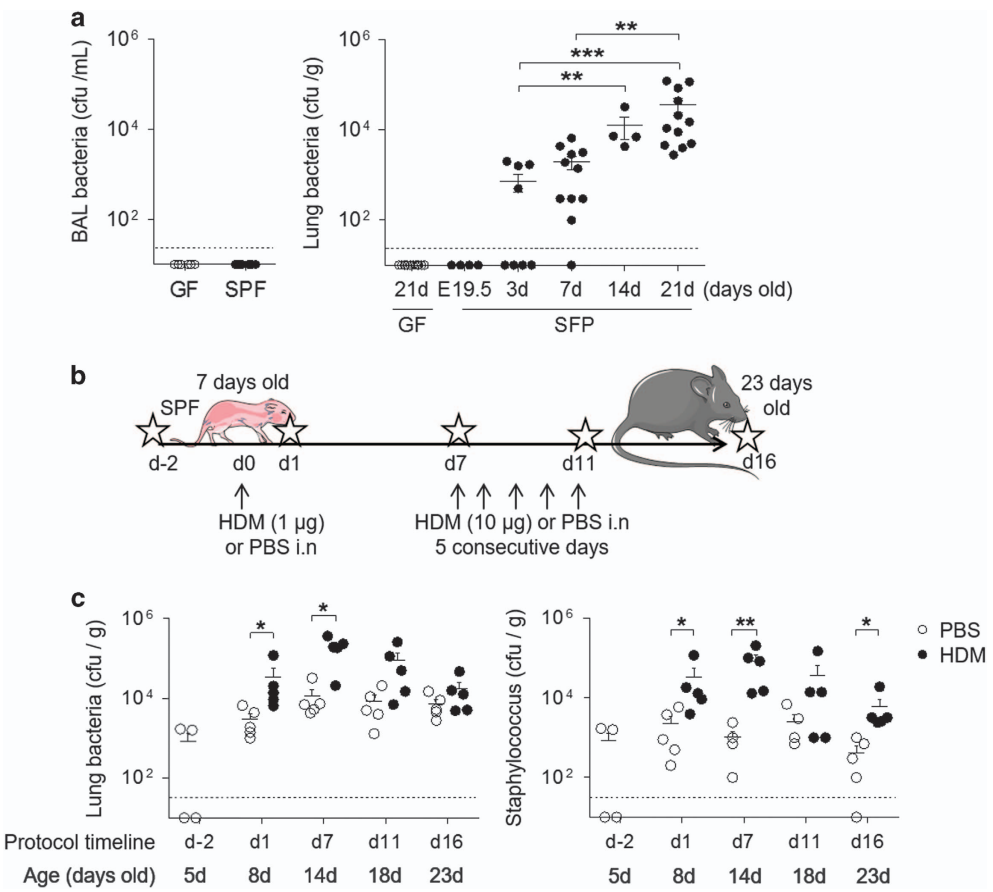

Figure 2 Lung microbiota is modified during HDM induced asthma. (**a**) BAL or lung homogenates were incubated 24 h on GyhBHI plates and the bacteria enumerated as colony-forming units (CFU per ml of BAL (from 21-day-old GF or SPF mice) or grams of lung (from embryonic day 19.5 embryos or 3, 7, 14 or 21-day-old neonates). (**b**) Schematic outline of the experimental approach for panel (**c**) (days of killing are illustrated with starts). (**c**) Lung homogenates were incubated 24 h on GyhBHI (to enumerate all bacteria CFU) and Mannitol Sel agar plates (to enumerate *Staphylococcus* CFU). (**a–c**) All data represent one of three independent experiments ($n=5$–10 mice per group).

To evaluate the impact of HDM treatment on the lung microbiota, mice were killed at different time points as illustrated by stars on the time line in Figure 2b. The number of bacteria recovered in non-selective GyhBHI medium significantly increased on d1 and d7 (Figure 2c, $P<0.05$). This tendency was not significant on d11, and the number of colony-forming units (CFU) reached similar levels for HDM and SPF mice on d16. *Staphylococci* levels were particularly high after HDM treatment (Figure 2c, selective Mannitol Sel Agar plates). Thus, HDM treatment influenced the composition of the lung microbiota during the neonatal period.

Lung bacteria influence asthma features

We next sought to screen the 20 lung bacterial strains for their capacity to differentially promote cytokine production by PCLS. Of the 20 strains tested, 7 induced significant production of cytokine (Supplementary Table S2) and CNCM I 4969 and CNCM I 4970 (patented strains, Gram$^+$ coccus) displayed specific immunostimulatory properties (Figure 3). After 24 h of co-culture with GF PCLS, CNCM I 4969 stimulated the secretion of IL-12p70 and decreased the basal level of TSLP (Figure 3, $P<0.01$). CNCM I 4970 significantly increased the amount of TLPS, IL-10, IL-17a and IL-12p70 released into PCLS supernatants (Figure 3, $P<0.001$ for TSLP, $P<0.01$ for IL-10 and IL-12p70, and $P<0.05$ for IL-17a). The secretion of IL-5 tends to be higher in CNCM I 4970-stimulated cells compared with non-stimulated cells, but does not reach significant level ($P=0.0625$). Altogether, CNCM I 4969 induced a type 1 cytokine profile whereas CNCM I 4970 (a member of the *Staphylococcus* genus, whose levels were higher after HDM treatment) induces secretion of the majority of cytokines tested (TSLP, IL-10, IL-17a and IL-12p70).

We next investigated whether these two immunomodulatory bacteria isolated from the neonatal lung microbiota could affect the severity of HDM-triggered asthma in SPF mice. Neonates received 10^6 CFU of CNCM I 4969 or CNCM I 4970 (10 µl intranasally every 2 days starting at d2), and the readouts of asthma features were explored after weaning in young adult mice (23 days old) as illustrated in Figure 4a. Nasal administration enabled bacterial delivery to the lungs, as verified by the detection of CFDA-SE labeled strains in BAL and lungs (Supplementary Figure S3). HDM treatment induced a small, but reproducible ($n=3$ experiments), growth delay in neonates (Figure 4b, PBS vs HDM, $P<0.001$). Indeed, during the challenge phase (d7 to d11), HDM-treated neonates gained less weight. CNCM I 4969 administered alone had no significant effect on the growth of the pups. CNCM I 4970 alone negatively affected weight gain (Figure 4b, PBS vs CNCM I 4970). This result was obtained for two of three experiments (data not shown). In the HDM groups, CNCM I 4969 protected the mice against the growth delay (Figure 4b, $P<0.001$) whereas CNCM I 4970 worsened it (Figure 4b, $P<0.05$). We observed fewer infiltrating cells in BAL from the CNCM I 4969+HDM group (Figure 5a, CNCM I 4969+HDM group vs HDM, $P<0.001$), and the percentage of eosinophils was lower (Figure 5a, $P<0.05$). The challenge with

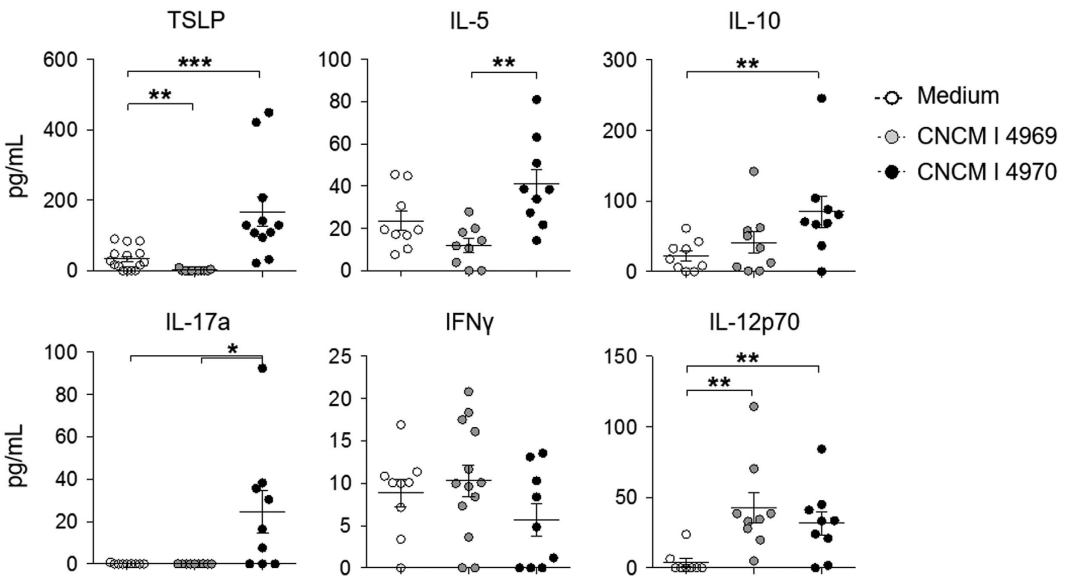

Figure 3 *Ex vivo* immunomodulation profiles of CNCM I 4969 and CNCM I 4970. Precision-cut lung slices (PCLS) of adult GF lungs were cultivated *ex vivo* for 24 h in supplemented RPMI alone (medium) or with 50 CFU of the two strains, CNCM I 4969 and CNCM I 4970, isolated from healthy neonatal lungs. Cytokines were measured in PCLS supernatants. Data represent two pooled independent experiments ($n=9$ mice per group). In total, four independent experiments were performed with similar results ($n=4$–5 mice per group per experiment).

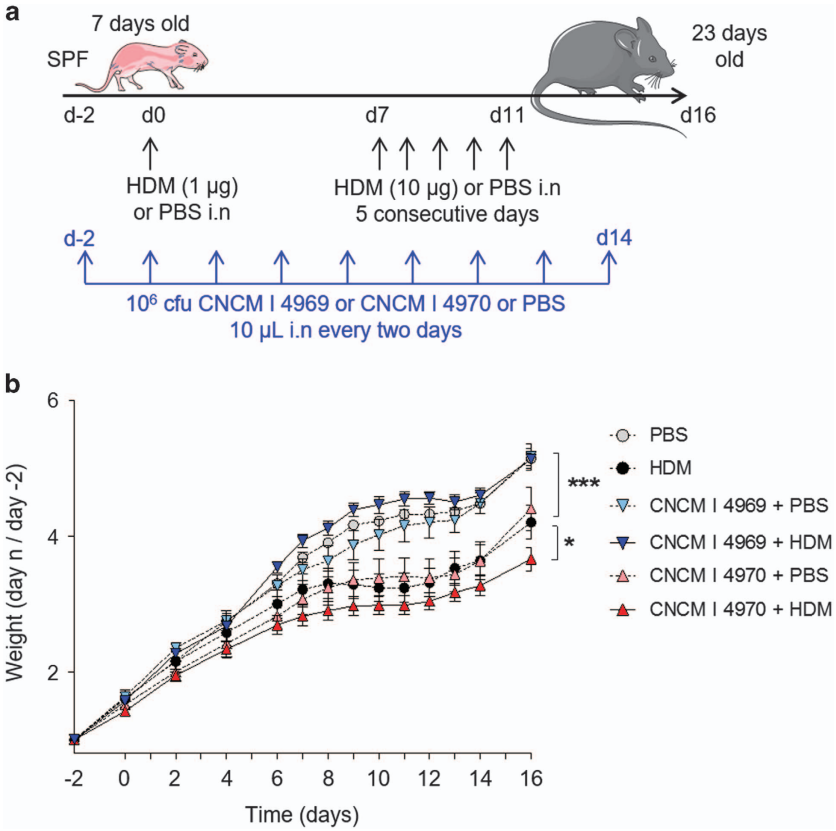

Figure 4 Bacterial intervention can modulate asthma features in SPF mice. (**a**) Schematic outline of the experimental approach. Animals were killed on d16. (**b**) Mice were weighed daily. The growth curves are expressed as the mean ± s.e.m. of individual weights (normalized to the initial weight on day -2) for $n \geqslant 5$ mice per group and represent one of three independent experiments ($n = 5$–10 mice per group). Tukey's multiple comparison test, repeated measures one-way ANOVA was used for comparison of the growth curves.

HDM increased the infiltration of neutrophils and lymphocytes (Figure 5a, $P<0.01$) that remained unchanged in the presence of our strains. The strains CNCM I 4970 significantly increased the basal level of neutrophils and lymphocytes (Figure 5a, PBS vs CNCM I 4970, $P<0.05$ and $P<0.01$). In our model, the response is due to eosinophil recruitment rather than neutrophil. CNCM I 4970 increased IL-5 levels in PBS-treated mice (Figure 5a, $P<0.05$) but they were similar in the HDM and CNCM I 4970+HDM groups. The basal level of IgE was increased by both strains, in the absence of HDM (Figure 5b, PBS vs CNCM I 4970 and PBS vs CNCM I 4969, $P<0.01$). The treatment with HDM led to a higher amount of serum IgE (Figure 5b, HDM vs PBS, $P<0.05$) and this HDM-induced IgE was worsened by CNCM I 4970 +HDM (Figure 5b, HDM vs CNCM I 4970+HDM, $P<0.01$). The serum IgE levels were not different in HDM and in CNCM I 4969+HDM, thus indicating that CNCM I 4969 has no impact on HDM-induced IgE. IgG1 levels were increased in the presence of HDM plus each strains (Figure 5b, HDM vs CNCM I 4970+HDM, $P<0.01$; HDM vs CNCM I 4969+HDM, $P<0.05$). In RLN supernatants, IL-5 and IL-10 production was significantly lower in the CNCM I 4969+HDM group than in the HDM group (Figure 5c, $P<0.05$), suggesting reduced type 2 immune priming.

The lungs from HDM-treated mice showed perivascular immune infiltrates, myofibroblast proliferation (Figure 6a, hematoxilin eosin safran staining), mucus production (Figure 6a, periodic acid schiff/alcian blue staining) and a thickened epithelium relative to PBS-treated mice (Figure 6b, $P<0.0001$). A similar pattern of inflammatory lesions was observed for the CNCM I 4970 group, which increased moderately upon HDM challenge. In contrast, CNCM I 4969 did not cause lung inflammation by itself and even reduced the extent of the inflammatory reaction in the tissue upon HDM challenge. All features were markedly reduced relative to the HDM or CNCM I 4970+HDM groups (Figures 6a and b, $P<0.0001$). Thus, inoculation with CNCM I 4969 protected mice from HDM-induced airway disease.

We obtained an intermediate profile when we co-administered CNCM I 4969 and CNCM I 4970. The mice were not protected against the growth delay (Figure 7a, HDM vs CNCM I 4969+4970+HDM = NS). Serum IgE and BAL IL-5 levels were similar (Figure 7b), but BAL cellularity was reduced ($10.39 \pm 0.45 \times 10^5$ in HDM vs $7.32 \pm 0.75 \times 10^5$ in CNCM I 4969+4970+HDM, $P<0.01$) as well as the percentage of BAL eosinophils (Figure 7b, $P<0.05$).

IL-5 levels were reduced in RLN supernatants after *in vitro* HDM re-stimulation (Figure 7c, $P<0.01$), reflecting reduced type 2 immune priming. Finally, histological examination of lung tissue revealed moderate inflammation, with a profile comparable to the HDM group (Figure 7d vs Figure 6). CNCM I 4969 appeared to attenuate some enhanced asthma features induced by CNCM I 4970 alone. Note that the strain CNCM I 4967 (*Lactobacillus* spp), also isolated from mouse lung, had neutral effect on HDM-

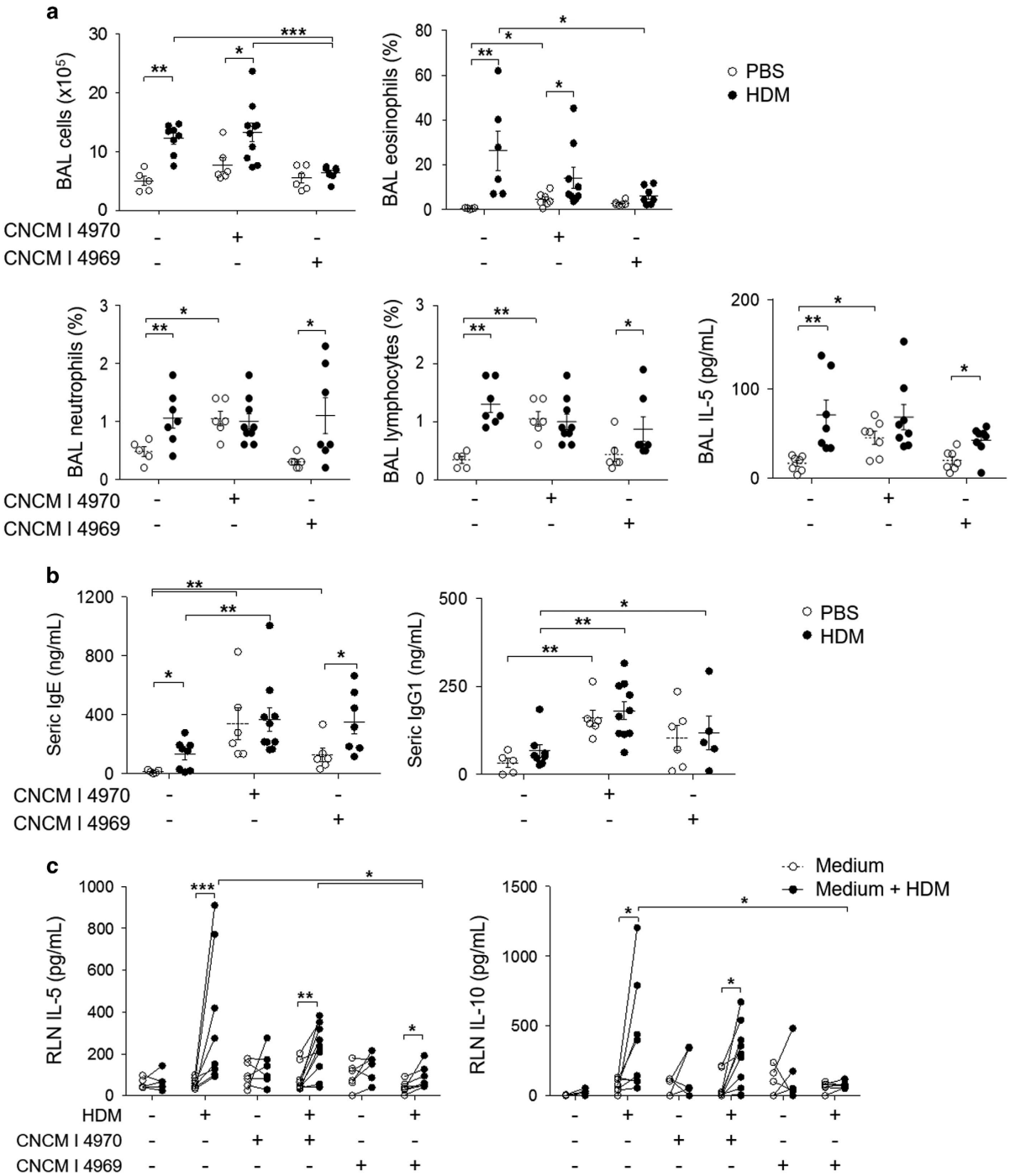

Figure 5 CNCM I 4969 decreases some type 2 immune features whereas CNCM I 4970 worsens it. SPF mice were treated as described in Figure 4. (**a**) BAL cells were enumerated, cytocentrifuged and stained with May–Gründwald–Giemsa. Eosinophils, neutrophils and lymphocytes were enumerated and expressed as the percentage of total BAL cells. BAL IL-5 levels were measured by enzyme-linked immunosorbent assay (ELISA). (**b**) Serum IgE and IgG1 levels were measured by ELISA. (**a**, **b**) Data are shown individually and as the mean ± s.e.m. (**c**) Individual respiratory lymph node (RLN) cells were isolated and cultivated 72 h in RPMI with or without HDM. IL-5 and IL-10 levels in the supernatants were measured by ELISA. The RPMI ± HDM values for the same mice are connected with a dotted line. (**a**–**c**) All data represent one of three independent experiments ($n = 5$–10 mice per group).

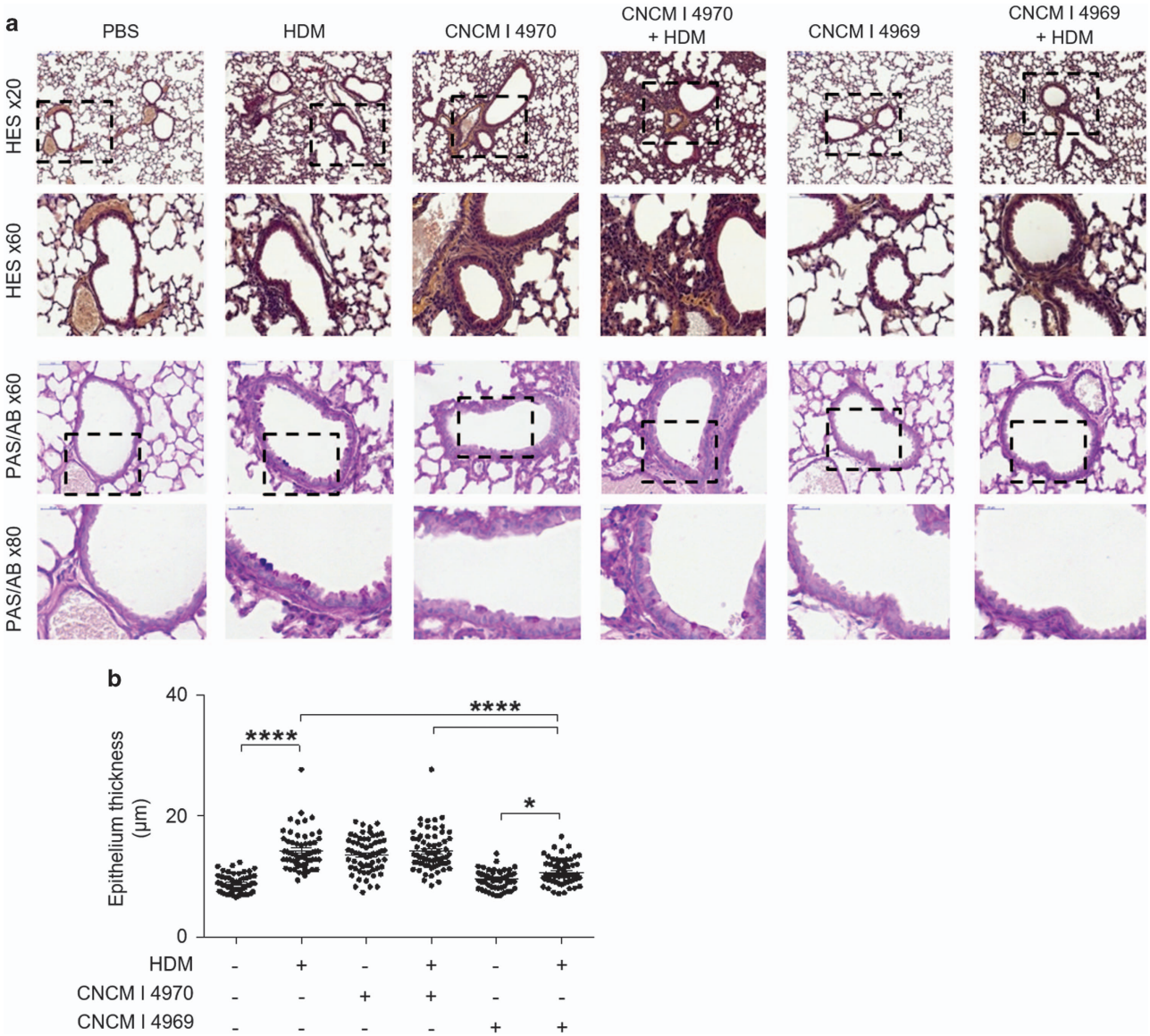

Figure 6 CNCM I 4969 protects against lung inflammation whereas CNCM I 4970 worsens it. SPF mice were treated as described in Figure 4. (**a**) Lung histology was assessed as described in Figure 1. Lung sections were stained with hematoxylin–eosin–saffron (HES, first two rows, enlargement × 20 and × 60) or periodic acid–Schiff and alcian blue (PAS/AB, bottom two rows, enlargement × 60 and × 80). One representative section per group is shown. (**b**) Epithelium thickness was measured using Case Viewer software. In total, 100 measures per group are plotted on the graph. They correspond to the analysis of four mice per group. Five representative bronchi were selected for each mouse and four measurements were performed per bronchus (up, down, left, right side). (**a**, **b**) All data represent one of two independent experiments ($n = 5$–10 mice per group).

induced asthma (Supplementary Table S2 and data not shown).

Altogether, our results show that forced inoculation of lung bacteria influences the severity of HDM-induced allergic asthma: CNCM I 4970 exacerbated some asthma features whereas CNCM I 4969 seemed to have a protective effect.

Discussion

Our study provides evidence for a reciprocal influence between lung bacteria and asthma in neonatal mice. Our data underline the bacterial hypothesis in asthma (Figure 8) as the early lung bacteria environment can worsen or attenuate asthma features.

We provide evidence for the presence of living bacteria in healthy mouse lungs. The number of viable bacteria increased slightly, but significantly, within the first 2 weeks. To our knowledge, only one other study has described the culture of living bacterial strains from adult mouse lungs (Yun *et al.*, 2014). In agreement with this study, we also found members of Enterobacteria and Firmicutes. Lung microbiota has been mostly investigated using genomic tools. Here, we used bacterial culture to further study the functional and immunomodulatory properties of lung bacteria.

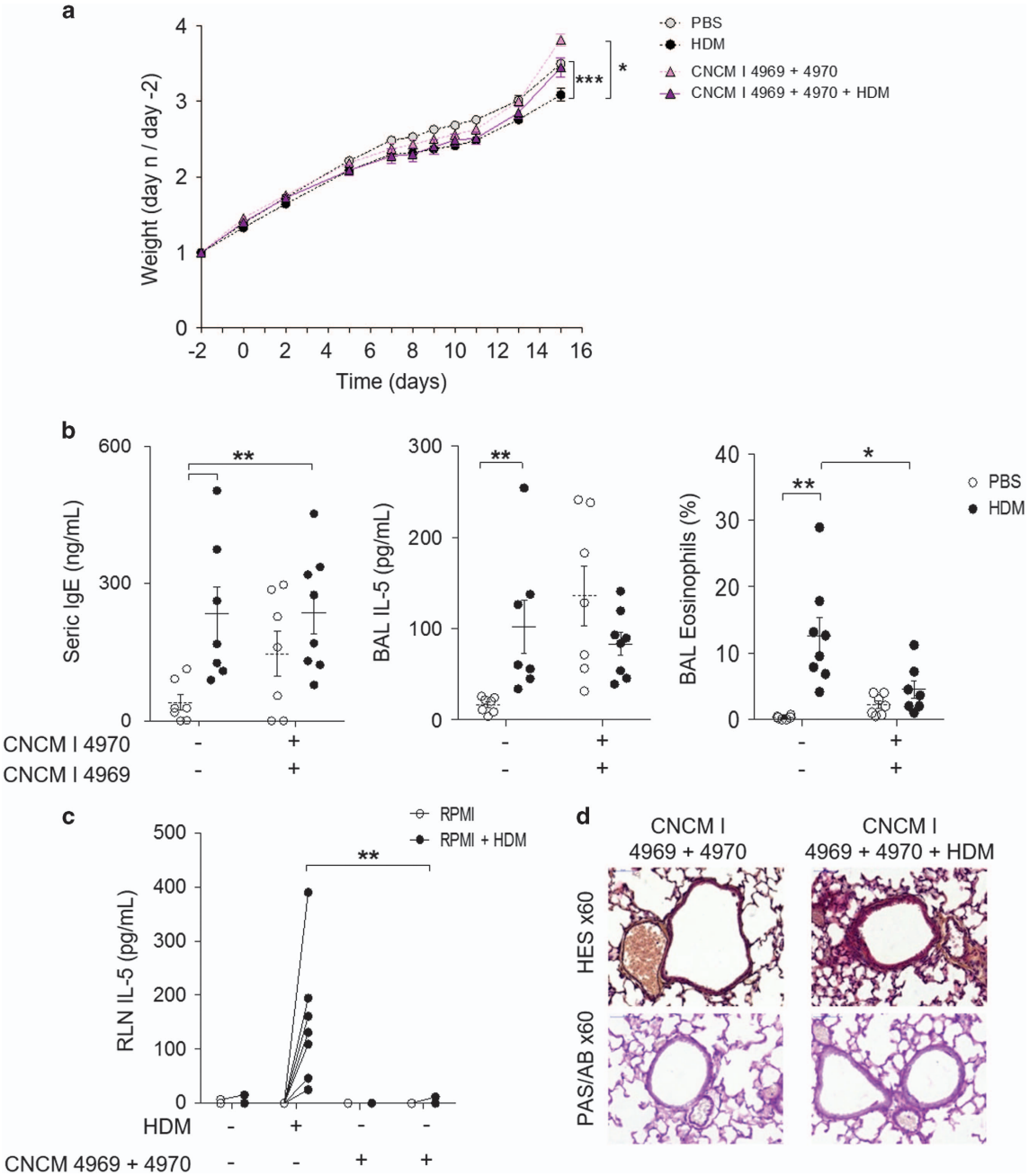

Figure 7 CNCM I 4969 and 4970 induce an intermediate inflammatory profile when given together. SPF mice were treated as described in Figure 4 but the two strains were inoculated together. (**a**) Mice were weighed daily. The growth curves are expressed as the mean ± s.e.m. of individual weights (normalized to initial weight at day -2). (**b**) Serum and BAL responses were analyzed as described in Figures 5a and b. Data are shown individually and as the mean ± s.e.m. (**c**) IL-5 was measured in RLN supernatants as described in Figure 5c. The RPMI ± HDM values for the same mice are connected with a dotted line. (**d**) Lung histology was assessed as described in Figure 1. Lung sections were stained with hematoxylin–eosin–saffron (HES) or Periodic acid–Schiff and alcian blue (PAS/AB). One representative section (enlargement × 60) per group is shown. (**a–d**) All data represent one experiment with $n = 7–8$ mice per group.

The presence of the microbiota obviously influences local lung physiology and immunity. We found that innate mRNA markers were differentially expressed at steady state between the lungs of GF and SPF mice and that BAL cellularity was higher is SPF mice. Histological examination of lung slices showed no major defect in the lungs of GF mice. On the contrary to what we observed in lung, the gut microbiota triggers extensive remodeling of the epithelium of the small and large intestines (El Aidy *et al.*, 2012; Tomas *et al.*, 2013; Hoffmann *et al.*, 2016). One important difference between gut and lung epithelia is their renewal, which is very active in the gut (Sancho *et al.*, 2004). The presence of stem and proliferative daughter cells allows constant reshaping of the gut to face a highly variable luminal

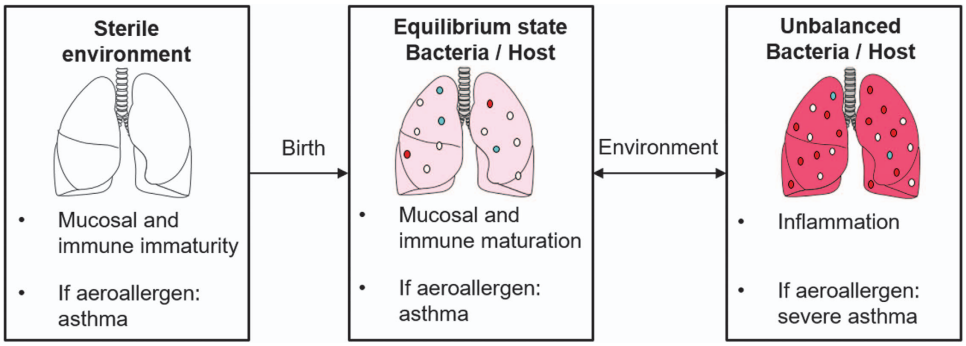

Figure 8 Lung microbiota is an early life determinant of susceptibility to allergic asthma. Lung bacteria environment affects lung physiology and immunity, and the equilibrium between the host and its microbiota influences microbiota composition and asthma features.

environment (Peifer, 2002; Joly *et al.*, 2009; Kaiko and Stappenbeck, 2014). For example, gut epithelial cell turnover is an efficient and effective mechanism for pathogen expulsion (Cliffe *et al.*, 2005). The low-level renewal of lung cells may be linked to the low influence of the microbiota on its structure.

The number of lung DC recovered from the lungs of GF and SPF mice in our experiments was similar, in agreement with Gollwitzer *et al.* (2014). These authors have also observed higher expression of CD40 and PD-L1 DC markers in 8-day-old SPF mice, showing a more mature phenotype in the presence of microbes. We have also found similar numbers of lung B and T lymphocytes, but did not assess the different helper T-cell subsets that have been shown to be regulated by the microbiota (Gollwitzer *et al.*, 2014; Ohnmacht *et al.*, 2015). Gollwitzer *et al.* (2014) reported no difference in lung DC and CD4 T cells frequency in GF and SPF mice following HDM exposure. In our hands, the same conclusion remained true (data not shown, one experiment).

GF mice have altered T- and B-cell numbers in the gut (Macpherson and Harris, 2004; Hooper and Macpherson, 2010). This is not the case in the lung. We hypothesize that lung regulatory mechanisms are less strongly affected by the microbiota, possibly due to a lower bacterial load: 10^{12} per gram in the colon (Costello *et al.*, 2009; Marchesi, 2011) vs 10^{4} per gram in the lung (Figure 3a). Some bacterial families specifically affect gut immunity and physiology (Wrzosek *et al.*, 2013; Miquel *et al.*, 2015b; Tomas *et al.*, 2015). For example, segmented filamentous bacteria increase Th17 (Lécuyer *et al.*, 2014). It is possible that family-specific regulation also occurs in the lung, as we observed different immune-regulating properties *ex vivo* of different bacterial strains.

Bacteria can be ranked into functional cores according to their function (Lozupone *et al.*, 2012) and it is well described that beneficial or detrimental effects of bacteria are specific to the strains considered (Miquel *et al.*, 2015a; Peres *et al.*, 2015). It may be instructive to link the effects of lung bacteria to their metabolic activity (Miquel *et al.*, 2015b). Indeed, we observed *in vitro* short-chain fatty acid production by the 20 strains that we studied: mainly acetate (5–60 mmol l^{-1}), and low levels of propionate and butyrate ($<$ 5 mmol l^{-1}) for some strains (data not shown). CNCM I 4969 and CNCN I 4970 produce the same amount of acetate (5–6 mmol l^{-1}) and no propionate or butyrate *in vitro* so it is unlikely that the difference observed on asthma pathology is due to a difference in short-chain fatty acid production.

The lung microbiota enters the airway within a few days and others have suggested that its composition stabilizes after 2–3 months in infants (Marsland, 2013). During this primocolonization process, the neonatal period represents a window of susceptibility to infections by pathogens, or the development of non-infectious diseases such as allergic asthma. Early and chronic exposure to microbial products such as endotoxin has been demonstrated to prevent allergic asthma in children growing up in a dairy farm (Schuijs *et al.*, 2015). Endotoxins reduce the production of DC-activating cytokines by epithelial cells, thus suppressing type 2 immunity to HDM (Schuijs *et al.*, 2015). Here, early administration of either pro-type 1 or pro-type 2 strains modulated aeroallergen responsiveness. Although we were able to reduce the type 2 immune response with CNCM I 4969, we did not observe increased production of type 1 cytokines IL-12p70 or IFNγ in RLN supernatants or BAL fluids (data not shown). TSLP levels in neonatal BAL fluids were under our detection limit. We also observed the presence of IL-17a in the CNCM I 4970 group samples, suggesting that this strain not only activated type 2 immunity but also the Th17 response. This was not the case for CNCM I 4969.

The administration of CNCM I 4969 or CNCM I 4970 in SPF mice did not change the frequency of lung DC and T cells observed after HDM challenge (data not shown, one experiment). The mechanism underpinning the CNCM I 4969 protective effects requires further investigations. When we inoculated CNCM I 4969 during the HDM challenge (d8) instead of before the sensitization (d2), we lost the protective effect of the strain (Supplementary Figure S4). We believe the timing for efficient CNCM I 4969-driven

attenuation to be crucial (Supplementary Figure S4). Our observations are in accordance with early life as a high susceptibility period for bacterial priming of the lung. The exploration of the influence of microbiota on lung immunity and the potential dysbiosis of microbial communities constitute a new and promising area of research, which will have an impact on the prevention and management of pulmonary diseases such as asthma.

Conflict of Interest

The authors declare no conflict of interest.

Acknowledgements

We thank Daphné Laubreton (INRA, Jouy-en-Josas, France), Gert Van Isterdael and Kim Deswarte (VIB, Gent) for assistance for the flow cytometry experiments. Staff from the three animal facilities, IERP and Anaxem (INRA) and the one at VIB (Ghent, Belgium), are gratefully acknowledged for taking proper care of the mice and for technical assistance. We also thank the Iso Cell Express platform (INRA) for access to the bioanalyzer. We thank Dr Genevieve Hery for Mass Spectrometry. Chantal Bridonneau and two bachelor's students, Alix Penel and Amélie Riou (Université Paris-Saclay), are warmly thanked for their help in several bacterial experiments. Dr Isabelle Schwartz-Cornil and Dr Claire Cherbuy are also acknowledged for their critical reading of the manuscript. Dr Aude Remot was supported by an Institut National de la Recherche Agronomique young scientist contract (CJS) and the UE in the framework of the Marie-Curie FP7 COFUND People Program, through the award of an Agreenskills fellowship under grant agreement number 267196. The Alimentation Humaine INRA division also supported the salary of AR. This work was funded by an IDEX prematuration grant from Université Paris-Saclay.

Author contributions

Conceptualization: AR, BL, PL, HH and MT; methodology: AR and AB; investigation: AR, DD, MLN, AB, VR, EM and MT; writing—original draft: AR and MT; writing—review and editing: AR, DD, SR, BL, PL, HH and MT; funding acquisition: AR, BL, PL, HH and MT; resources: AB, BL, SR, PL, HH and MT; supervision: AR, HH and MT; project administration: AR, HH and MT.

References

Bassis C, Erb-Downward J, Dickson R, Freeman C, Schmidt T, Young V *et al.* (2015). Analysis of the upper respiratory tract microbiotas as the source of the lung and gastric microbiotas in healthy individuals. *MBio* **6**: e00037.

Beck JM, Young VB, Huffnagle GB. (2012). The microbiome of the lung. *Transl Res* **160**: 258–266.

Buffie C, Pamer E. (2013). Microbiota-mediated colonization resistance against intestinal pathogens. *Nat Rev Immunol* **13**: 790–801.

Cahenzli J, Köller Y, Wyss M, Geuking M, Mccoy K. (2013). Intestinal microbial diversity during early-life colonization shapes long-term IgE levels. *Cell Host Microbe* **14**: 559–570.

Cerf-Bensussan N, Gaboriau-Routhiau V. (2010). The immune system and the gut microbiota: friends or foes? *Nat Rev Immunol* **10**: 735–744.

Charlson ES, Bittinger K, Chen J, Diamond JM, Li H, Collman RG *et al.* (2012). Assessing bacterial populations in the lung by replicate analysis of samples from the upper and lower respiratory tracts. *PLoS One* **7**: e42786.

Charlson ES, Bittinger K, Haas AR, Fitzgerald AS, Frank I, Yadav A *et al.* (2011). Topographical continuity of bacterial populations in the healthy human respiratory tract. *Am J Respir Crit Care Med* **184**: 957–963.

Cherbuy C, Honvo-Houeto E, Bruneau A, Bridonneau C, Mayeur C, Duée P-H *et al.* (2010). Microbiota matures colonic epithelium through a coordinated induction of cell cycle-related proteins in gnotobiotic rat. *Am J Physiol Gastrointest Liver Physiol* **299**: G348–G357.

Cliffe L, Humphreys N, Lane T, Potten C, Booth C, Grencis R. (2005). Accelerated intestinal epithelial cell turnover: a new mechanism of parasite expulsion. *Science* **308**: 1463–1465.

Costello E, Lauber C, Hamady M, Fierer N, Gordon J, Knight R. (2009). Bacterial community variation in human body habitats across space and time. *Science* **326**: 169467.

De Filippo C, Cavalieri D, Di Paola M, Ramazzotti M, Poullet J, Massart S *et al.* (2010). Impact of diet in shaping gut microbiota revealed by a comparative study in children from Europe and rural Africa. *Proc Natl Acad Sci USA* **107**: 14691–14696.

El Aidy S, Van Baarlen P, Derrien M, Lindenbergh-Kortleve D, Hooiveld G, Levenez F *et al.* (2012). Temporal and spatial interplay of microbiota and intestinal mucosa drive establishment of immune homeostasis in conventionalized mice. *Mucosal Immunol* **5**: 567–579.

Erb-Downward JR, Thompson DL, Han MK, Freeman CM, Mccloskey L, Schmidt LA *et al.* (2011). Analysis of the lung microbiome in the ''healthy'' smoker and in COPD. *PloS One* **6**: e16384.

Fujimura K, Lynch S. (2015). Microbiota in allergy and asthma and the emerging relationship with the gut microbiome. *Cell Host Microbe* **17**: 592–602.

Gaboriau-Routhiau V, Rakotobe S, Lécuyer E, Mulder I, Lan A, Bridonneau C *et al.* (2009). The key role of segmented filamentous bacteria in the coordinated maturation of gut helper T cell responses. *Immunity* **31**: 677–689.

Goleva E, Jackson L, Harris J, Robertson C, Sutherland E, Hall C *et al.* (2013). The effects of airway microbiome on corticosteroid responsiveness in asthma. *Am J Respir Crit Care Med* **188**: 1193–1201.

Gollwitzer E, Saglani O, Trompette A, Yadava K, Sherburn R, Mccoy K *et al.* (2014). Lung microbiota promotes tolerance to allergens in neonates via PD-L1. *Nat Med* **20**: 642–647.

Herbst T, Sichelstiel A, Schär C, Yadava K, Bürki K, Cahenzli J *et al.* (2011). Dysregulation of allergic airway inflammation in the absence of microbial colonization. *Am J Respir Crit Care Med* **184**: 198–205.

Hill D, Siracusa M, Abt M, Kim B, Kobuley D, Kubo M *et al.* (2012). Commensal bacteria-derived signals regulate basophil hematopoiesis and allergic inflammation. *Nat Med* **18**: 538–546.

Hilty M, Burke C, Pedro H, Cardenas P, Bush A, Bossley C *et al.* (2010). Disordered Microbial Communities in Asthmatic Airways. *PLoS One* **5**: e8578.

Hoffmann T, Pham H, Bridonneau C, Aubry C, Lamas B, Martin-Gallausiaux C *et al.* (2016). Microorganisms linked to inflammatory bowel disease-associated dysbiosis differentially impact host physiology in gnotobiotic mice. *ISME J* **10**: 460–477.

Hooper L, Macpherson A. (2010). Immune adaptations that maintain homeostasis with the intestinal microbiota. *Nat Rev Immunol* **10**: 159–169.

Hoskin-Parr L, Teyhan A, Blocker A, Henderson AJ. (2013). Antibiotic exposure in the first two years of life and development of asthma and other allergic diseases by 7.5 yr: a dose-dependent relationship. *Pediatr Allergy Immunol* **24**: 762–771.

Huang Y, Nariya S, Harris J, Lynch S, Choy D, Arron J *et al.* (2015). The airway microbiome in patients with severe asthma: Associations with disease features and severity. *J Allergy Clin Immunol* **136**: 874–884.

Joly F, Mayeur C, Messing B, Lavergne-Slove A, Cazals-Hatem D, Noordine M *et al.* (2009). Morphological adaptation with preserved proliferation/transporter content in the colon of patients with short bowel syndrome. *Am J Physiol Gastrointest Liver Physiol* **297**: 116–123.

Just J, Saint-Pierre P, Gouvis-Echraghi R, Laoudi Y, Roufai L, Momas I *et al.* (2014). Childhood allergic asthma is not a single phenotype. *J Pediatr* **164**: 815–820.

Kaiko G, Stappenbeck T. (2014). Host-microbe interactions shaping the gastrointestinal environment. *Trends Immunol* **35**: 538–548.

Kool M, Hammad H, Lambrecht BN. (2012). Cellular networks controlling Th2 polarization in allergy and immunity. *F1000 Biol Rep* **4**: 6.

Lécuyer E, Rakotobe S, Lengliné-Garnier H, Lebreton C, Picard M, Juste C *et al.* (2014). Segmented filamentous bacterium uses secondary and tertiary lymphoid tissues to induce gut IgA and specific T helper 17 cell responses. *Immunity* **40**: 608–620.

Lozupone C, Stombaugh J, Gordon J, Jansson J, Knight R. (2012). Diversity, stability and resilience of the human gut microbiota. *Nature* **489**: 220–230.

Macpherson A, Harris N. (2004). Interactions between commensal intestinal bacteria and the immune system. *Nat Rev Immunol* **4**: 478–485.

Marchesi J. (2011). Human distal gut microbiome. *Environ Microbiol* **13**: 3088–3102.

Marsland B. (2013). Influences of the microbiome on the early origins of allergic asthma. *Ann Am Thorac Soc* **10**(Suppl): S165–S169.

Miquel S, Beaumont M, Martin R, Langella P, Braesco V, Thomas M. (2015a). A proposed framework for an appropriate evaluation scheme for microorganisms as novel foods with a health claim in Europe. *Microb Cell Fact* **14**: 48.

Miquel S, Leclerc M, Martin R, Chain F, Lenoir M, Raguideau S *et al.* (2015b). Identification of metabolic signatures linked to anti-inflammatory effects of Faecalibacterium prausnitzii. *MBio* **6**: e00300–e00315.

Noverr MC, Huffnagle GB. (2005). The 'microflora hypothesis' of allergic diseases. *Clin Exp Allergy* **35**: 1511–1520.

Noverr MC, Noggle RM, Toews GB, Huffnagle GB. (2004). Role of antibiotics and fungal microbiota in driving pulmonary allergic responses. *Infect Immunity* **72**: 4996–5003.

Ohnmacht C, Park J, Cording S, Wing J, Atarashi K, Obata Y *et al.* (2015). The microbiota regulates type 2 immunity through RORγt + T cells. *Science* **349**: 989–993.

Olszak T, An D, Zeissig S, Vera MP, Richter J, Franke A *et al.* (2012). Microbial exposure during early life has persistent effects on natural killer T cell function. *Science* **336**: 489–493.

Peifer M. (2002). Developmental biology: colon construction. *Nature* **420**: 274–275.

Peres AG, Stegen C, Li J, Xu AQ, Levast B, Surette MG *et al.* (2015). Uncoupling of pro- and anti-inflammatory properties of Staphylococcus aureus. *Infect Immun* **83**: 1587–1597.

Plantinga M, Guilliams M, Vanheerswynghels M, Deswarte K, Branco-Madeira F, Toussaint W *et al.* (2013). Conventional and monocyte-derived CD11b(+) dendritic cells initiate and maintain T helper 2 cell-mediated immunity to house dust mite allergen. *Immunity* **38**: 322–335; S1074-7613, 00004-6.

Roux X, Remot A, Petit-Camurdan A, Nahori MA, Kiefer-Biasizzo H, Marchal G *et al.* (2011). Neonatal lung immune responses show a shift of cytokines and transcription factors toward Th2 and a deficit in conventional and plasmacytoid dendritic cells. *Eur J Immunol* **41**: 2852–2861.

Sancho E, Batlle E, Clevers H. (2004). Signaling pathways in intestinal development and cancer. *Annu Rev Cell Dev Biol* **20**: 695–723.

Schuijs M, Willart M, Vergote K, Gras D, Deswarte K, Ege M *et al.* (2015). Farm dust and endotoxin protect against allergy through A20 induction in lung epithelial cells. *Science* **349**: 1106–1110.

Segal L, Alekseyenko A, Clemente J, Kulkarni R, Wu B, Gao Z *et al.* (2013). Enrichment of lung microbiome with supraglottic taxa is associated with increased pulmonary inflammation. *Microbiome* **1**: 19.

Sibley CD, Grinwis ME, Field TR, Eshaghurshan CS, Faria MM, Dowd SE *et al.* (2011). Culture enriched molecular profiling of the cystic fibrosis airway microbiome. *PLoS One* **6**: e22702.

Smits H, Hiemstra P, Prazeres Da Costa C, Ege M, Edwards M, Garn H *et al.* (2016). Microbes and asthma: opportunities for intervention. *J Allergy Clin Immunol* **137**: 690–697.

Teo S, Mok D, Pham K, Kusel M, Serralha M, Troy N *et al.* (2015). The infant nasopharyngeal microbiome impacts severity of lower respiratory infection and risk of asthma development. *Cell Host Microbe* **17**: 704–715.

Tomas J, Reygner J, Mayeur C, Ducroc R, Bouet S, Bridonneau C *et al.* (2015). Early colonizing Escherichia coli elicits remodeling of rat colonic epithelium shifting toward a new homeostatic state. *ISME J* **9**: 46–58.

Tomas J, Wrzosek L, Bouznad N, Bouet S, Mayeur C, Noordine M *et al.* (2013). Primocolonization is associated with colonic epithelial maturation during conventionalization. *FASEB J* **27**: 645–655.

Venkataraman A, Bassis C, Beck J, Young V, Curtis J, Huffnagle G *et al.* (2015). Application of a neutral community model to assess structuring of the human lung microbiome. *MBio* **6**: e02284–14.

Wills-Karp M, Santeliz J, Karp CL. (2001). The germless theory of allergic disease: revisiting the hygiene hypothesis. *Nat Rev Immunol* **1**: 69–75.

Wrzosek L, Miquel S, Noordine M, Bouet S, Chevalier-Curt M, Robert V *et al.* (2013). Bacteroides thetaiotaomicron and Faecalibacterium prausnitzii influence the production of mucus glycans and the development of goblet cells in the colonic epithelium of a gnotobiotic model rodent. *BMC Biol* **11**: 61.

Yun Y, Srinivas G, Kuenzel S, Linnenbrink M, Alnahas S, Bruce K *et al.* (2014). Environmentally determined differences in the murine lung microbiota and their relation to alveolar architecture. *PLoS One* **9**: e113466.

This work is licensed under a Creative Commons Attribution-NonCommercial-NoDerivs 4.0 International License. The images or other third party material in this article are included in the article's Creative Commons license, unless indicated otherwise in the credit line; if the material is not included under the Creative Commons license, users will need to obtain permission from the license holder to reproduce the material. To view a copy of this license, visit http://creativecommons.org/licenses/by-nc-nd/4.0/

Supplementary Information accompanies this paper on The ISME Journal website (http://www.nature.com/ismej)

Figure S1

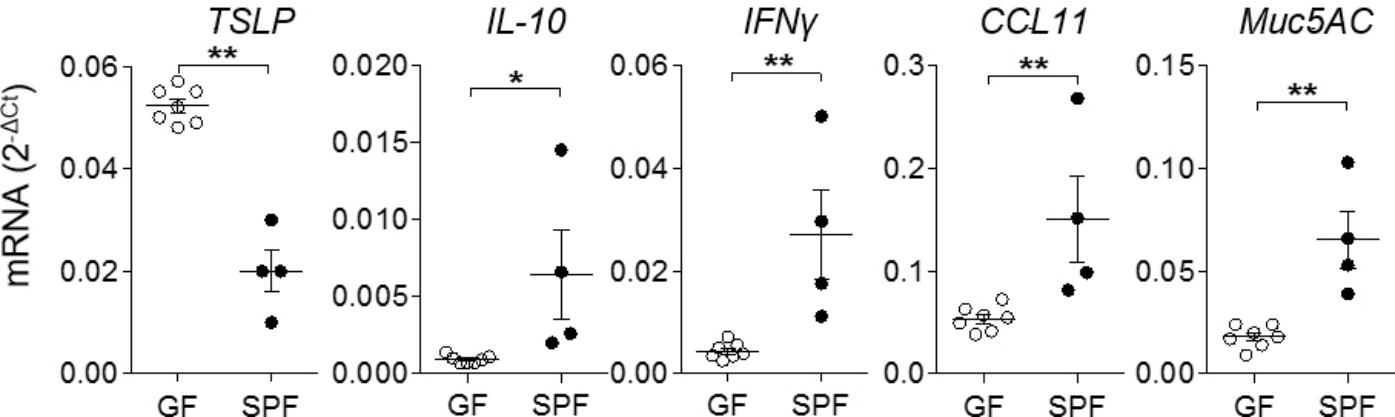
TSLP
IL-10
IFNγ
CCL11
Muc5AC
mRNA (2^-ΔCt)
0.06
0.04
0.02
0.00
0.020
0.015
0.010
0.005
0.000
0.3
0.2
0.1
0.0
0.15
0.10
0.05
**
*
GF
SPF

Figure S2

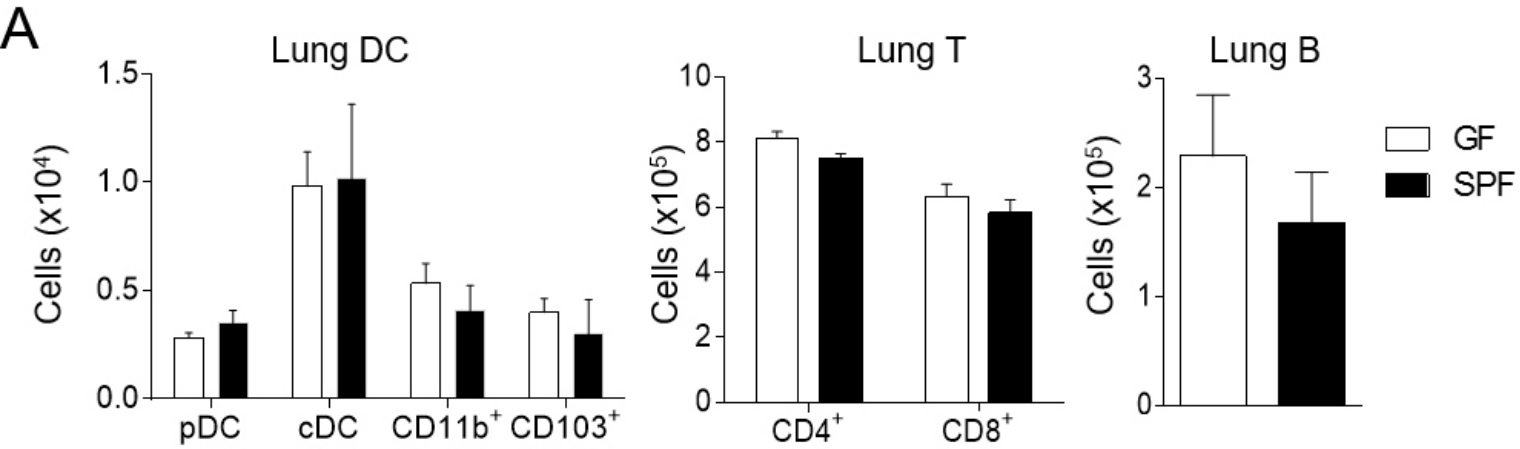
A
Lung DC
Lung T
Lung B
Cells (x10⁴)
Cells (x10⁵)
Cells (x10⁵)
pDC
cDC
CD11b⁺
CD103⁺
CD4⁺
CD8⁺
GF
SPF

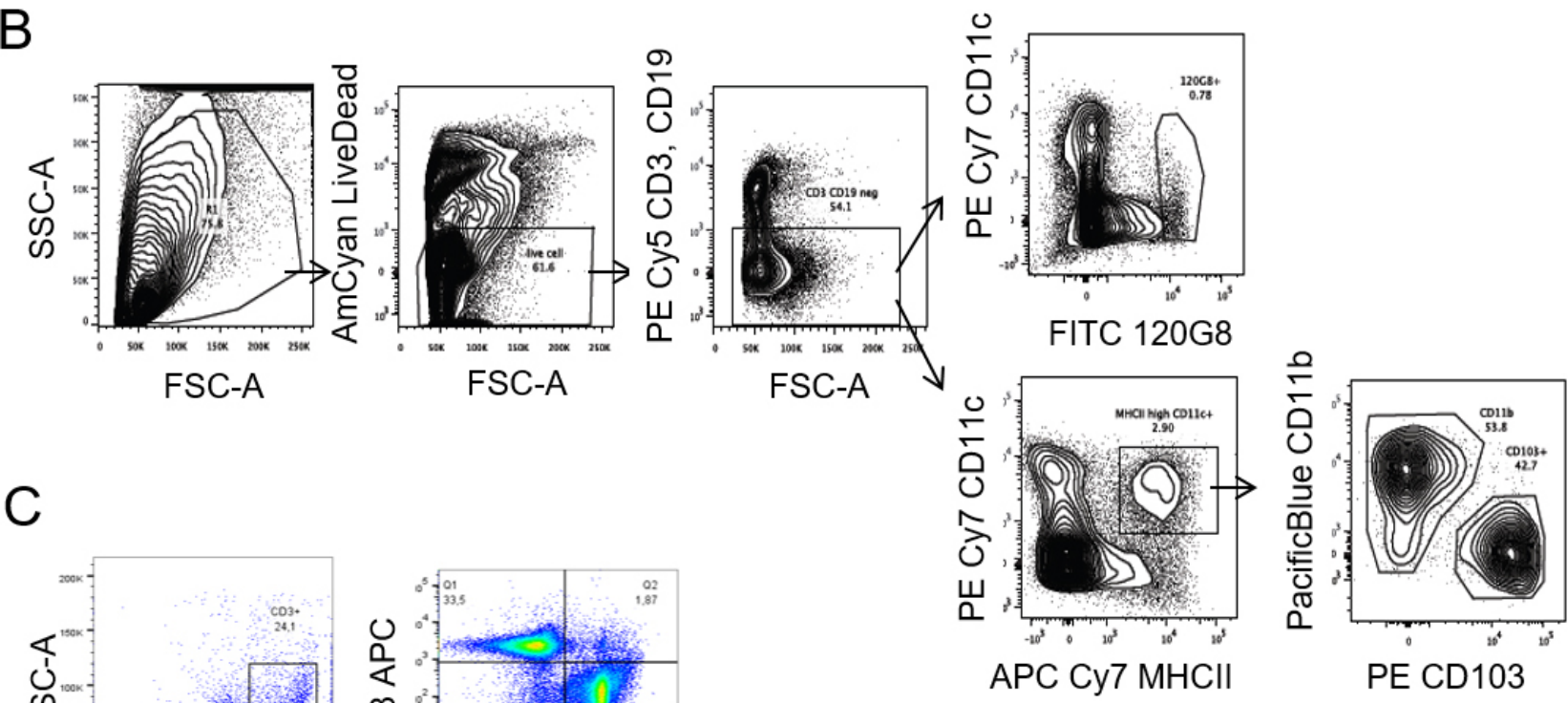
B
SSC-A
FSC-A
AmCyan LiveDead
FSC-A
PE Cy5 CD3, CD19
FSC-A
PE Cy7 CD11c
FITC 120G8
PE Cy7 CD11c
APC Cy7 MHCII
PacificBlue CD11b
PE CD103

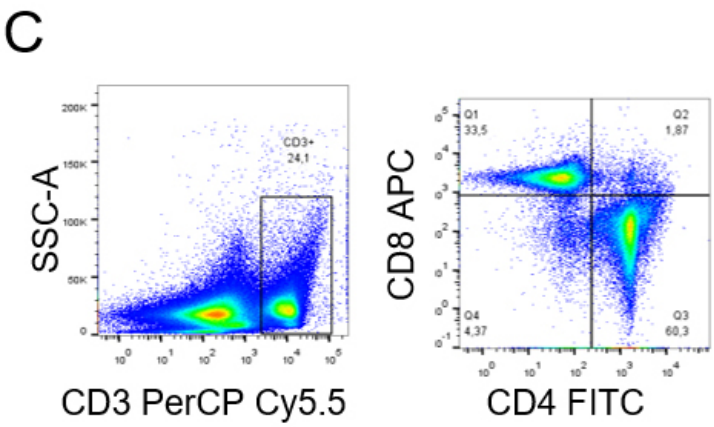
C
SSC-A
CD3 PerCP Cy5.5
CD8 APC
CD4 FITC

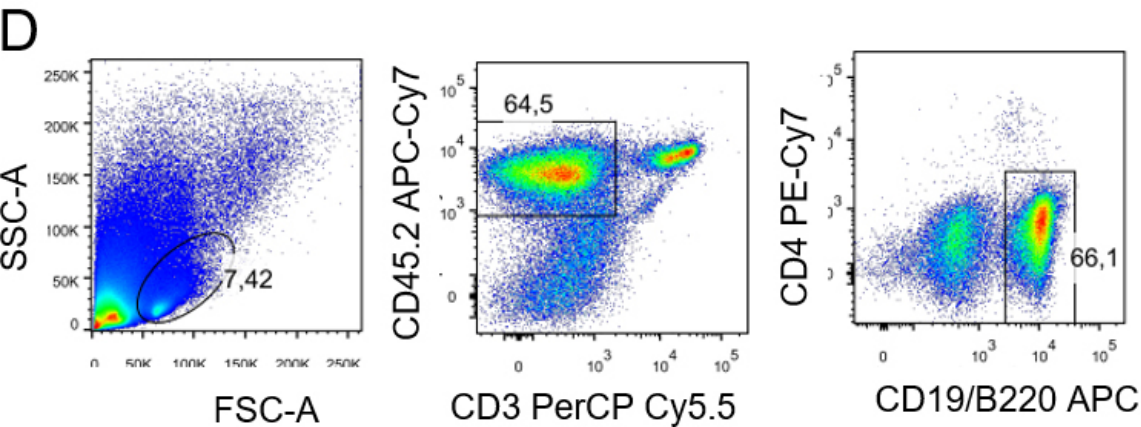
D
SSC-A
7,42
FSC-A
CD45.2 APC-Cy7
64,5
CD3 PerCP Cy5.5
CD4 PE-Cy7
66,1
CD19/B220 APC

Figure S3

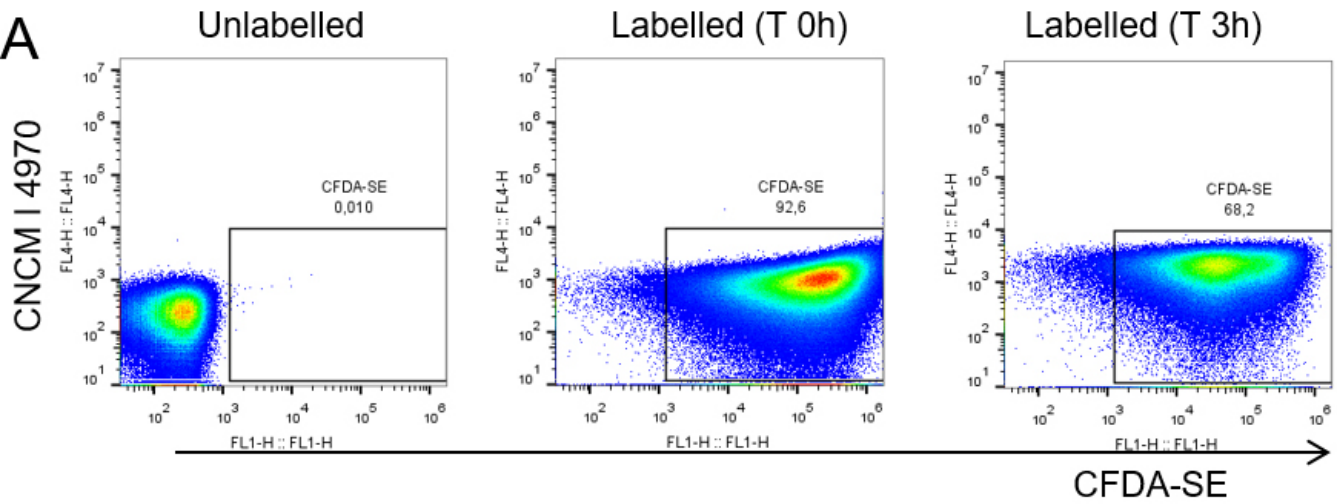
A
Unlabelled
Labelled (T 0h)
Labelled (T 3h)
CNCM I 4970
CFDA-SE
0,010
CFDA-SE
92,6
CFDA-SE
68,2
FL4-H :: FL4-H
FL1-H :: FL1-H
CFDA-SE

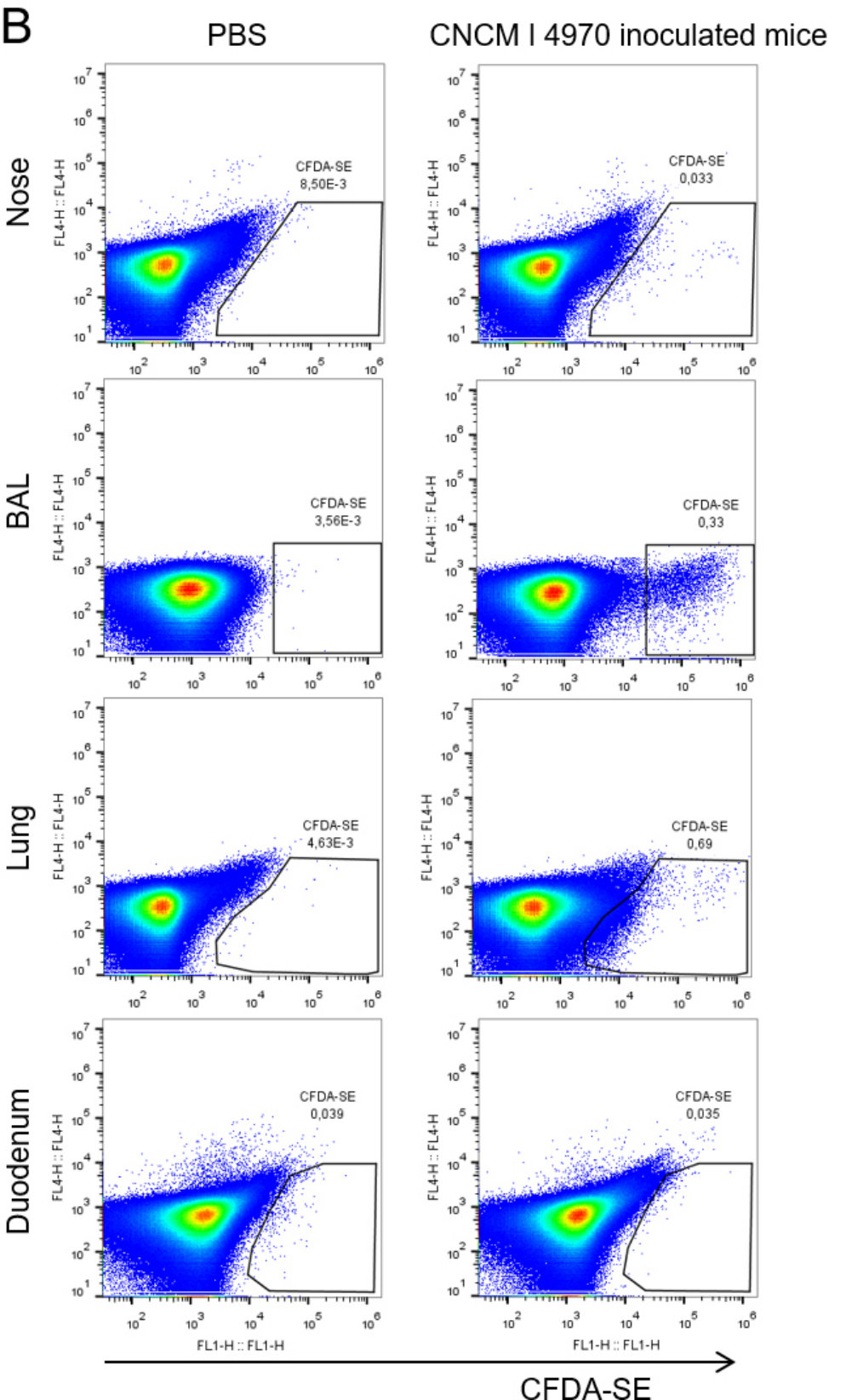
B
PBS
CNCM I 4970 inoculated mice
Nose
BAL
Lung
Duodenum
CFDA-SE
8,50E-3
CFDA-SE
0,033
CFDA-SE
3,56E-3
CFDA-SE
0,33
CFDA-SE
4,63E-3
CFDA-SE
0,69
CFDA-SE
0,039
CFDA-SE
0,035
FL4-H :: FL4-H
FL1-H :: FL1-H
CFDA-SE

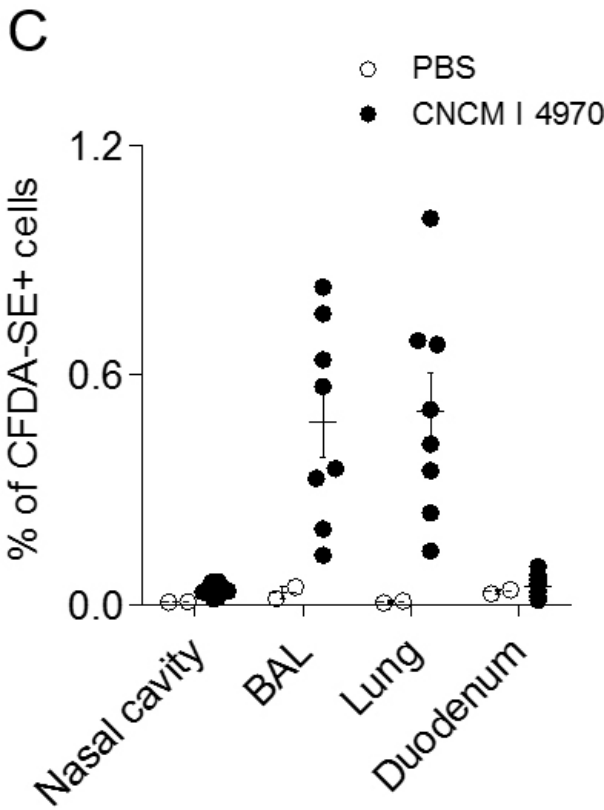
C
PBS
CNCM I 4970
% of CFDA-SE+ cells
1.2
0.6
0.0
Nasal cavity
BAL
Lung
Duodenum

Figure S4

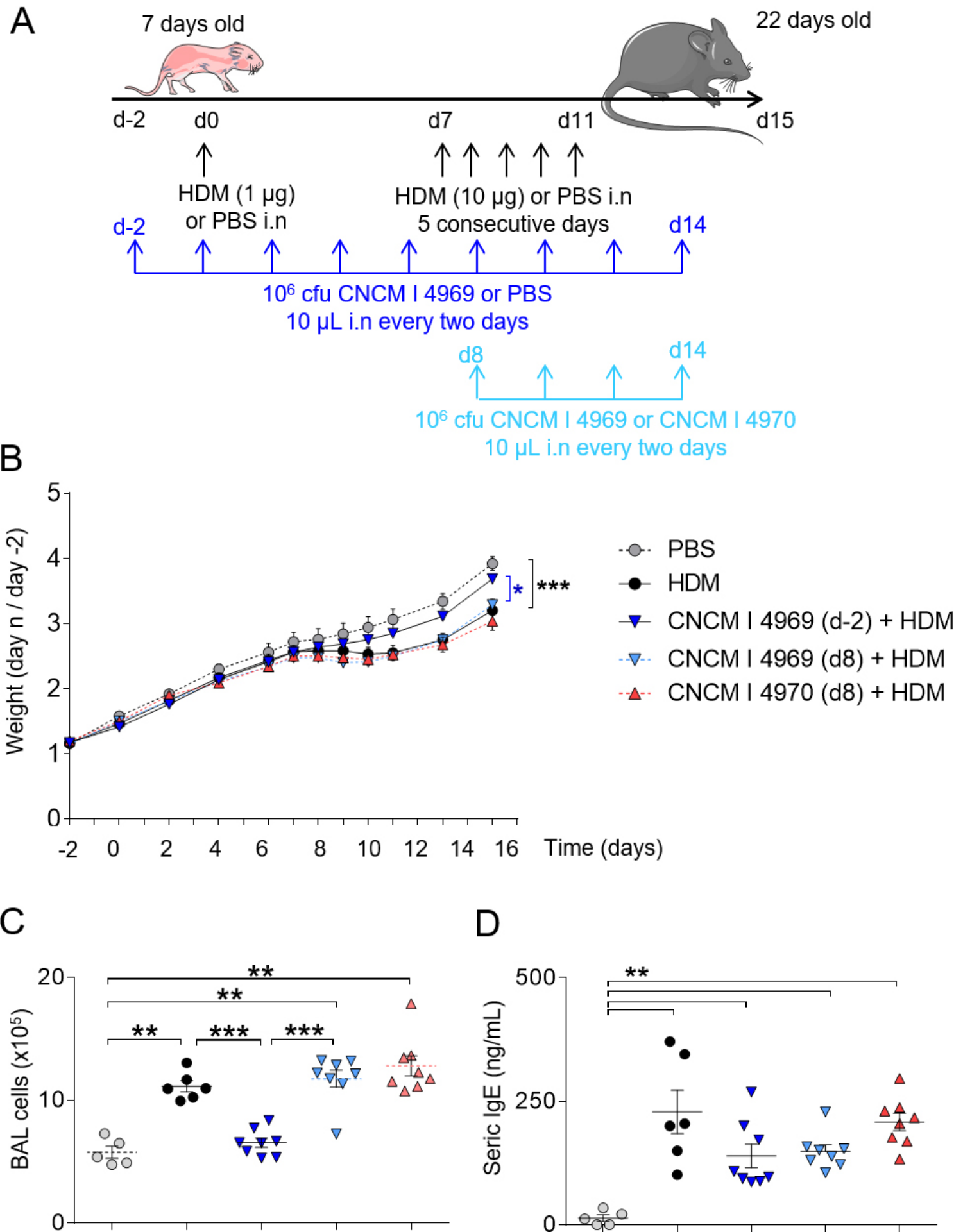
A
7 days old
22 days old
d-2
d0
d7
d11
d15
HDM (1 µg)
or PBS i.n
HDM (10 µg) or PBS i.n
5 consecutive days
d-2
d14
10⁶ cfu CNCM I 4969 or PBS
10 µL i.n every two days
d8
d14
10⁶ cfu CNCM I 4969 or CNCM I 4970
10 µL i.n every two days
B
Weight (day n / day -2)
Time (days)
PBS
HDM
CNCM I 4969 (d-2) + HDM
CNCM I 4969 (d8) + HDM
CNCM I 4970 (d8) + HDM
C
BAL cells (x10⁵)
D
Seric IgE (ng/mL)

Supplementary Table 1 : List of q-RT-PCR primers

Name of gene	Forward primer (5’ to 3’)	Reverse primer (5’ to 3’)
mHPRT	CAGGCCAGACTTTGTTGGAT	TTGCGCTCATCTTAGGCTTT
TSLP	GCCATTTCCTGAGTACCGTC	TTCACTCCCCGACAAAACAT
IL-10	TGGCCTTGTAGACACCTTGG	AGCTGAAGACCCTCAGGATG
IFNg	GCGTCATTGAATCACACCTG	GAGCTCATTGAATGCTTGGC
CCL11	TAAAGCAGCAGGAAGTTGGG	CATCTGTCTCCCTCCACCAT
Muc5AC	CCAGCACCATCTCTACAACCC	GCAAAGCTCCTGTTTGCACTC

Table S2: Descriptive table of the 20 isolated mouse lung strains

						significative *ex vivo* effect (co-culture with GF lung explants, PCLS)		significative *in vivo* effect (HDM model)
	Familly	**species**	**Gram**	**Catalase**	**Methode of identification**	**increase**	**decrease**	
1	*Staphylococcaceae*	*sciuri* (**CNCM I 4970**)	+	+	16S Sequencing, API Staph, Mass spectrometry	IL-5, IL-10, IL-12p70, IL-17a, TSLP	-	exacerbative
2		*aureus*	+	+	16S Sequencing, API Staph	*Non significant*		
3		*lugdunensis*	+	+	16S Sequencing, API Staph	IL-4, IL-17a, TSLP	-	
4		*haemoliticus*	+	+	16S Sequencing, API Staph	*Non significant*		
5		*xylosus*	+	+	16S Sequencing, API Staph	*Non significant*		
6		*epidermidis*	+	+	16S Sequencing, API Staph	*Non significant*		
7		*pasteuri*	+	+	16S Sequencing	*Non significant*		
8		*lentus*	+	+	16S Sequencing	*Non significant*		
9	*Streptococcaceae*	*dysgalactiae*	+	-	16S Sequencing, API20Strep	*Non significant*		
10		*salivarius*	+	-	16S Sequencing, API20Strep	*Non significant*		
11		*mitis / spp*	+	-	16S Sequencing	*Non significant*		
12	*Enterococcaceae*	*faecalis* (**CNCM I 4969**)	+	-	16S Sequencing, API20Strep, Mass spectrometry	IL-12p70	TSLP	protective
13		*spp/ haemoperoxidus*	+	-	16S Sequencing	*Non significant*		
14	*Lactobacillaceae*	*rhamnosus/spp* (**CNCM I 4967**)	+	-	16S Sequencing, Mass spectrometry	IL-10, IL-12p70, IFNg	-	no effect
15		*salivarius/spp* (**CNCM I 4968**)	+	-	16S Sequencing, Mass spectrometry	IL-4, IL-5, IL-12p70, IL-17a, IFNg	-	
16		*animalis/spp*	+	-	16S Sequencing	*Non significant*		
17	Clostridiacaea	*Clostridium/ spp*	+	-	16S Sequencing	*Non significant*		
18	*Enterobacteriaceae*	*E. coli*	-	+	16S Sequencing, API20E	IL-17a, IFNg	-	
19		*Proteus mirabilis*	-	+	16S Sequencing, API20E	IL-6, TNFa, IFNg, TSLP	-	
20	*Listeriaceae*	*Listeria spp*	-	+	16S Sequencing	*Non significant*		